ISSN 0027-1349, Moscow University Physics Bulletin, 2015, Vol. 70, No. 5, pp. 411–415. © Allerton Press, Inc., 2015.
Original Russian Text © O.Yu. Nishchak, N.F. Savchenko, V.V. Khvostov, 2015, published in Vestnik Moskovskogo Universiteta. Fizika, 2015, No. 5, pp. 81–85.

CONDENSED MATTER PHYSICS

The Structure and Electrochemical Properties of Nanocarbon Material

O. Yu. Nishchak, N. F. Savchenko, and V. V. Khvostov

Department of Physics, Moscow State University, Moscow, 119991 Russia

e-mail: nishchak@physics.msu.ru

Received June 5, 2015; in final form, July 7, 2015

Abstract—Nanocarbon material prepared via dehydrohalogenation of PVC-PVDC copolymer was studied in this work. The results of structural characterization of this material reveal the growth in the chain component fraction with increasing temperature of annealing that increases the specific capacity from 5 to 25 F/g. Chemical activation results in a noticeable growth of the specific capacity to 100 F/g.

Keywords: nanocarbon, Raman spectroscopy, electron spectroscopy, energy-storage elements, supercapacitor.

DOI: 10.3103/S0027134915050112

INTRODUCTION

Existing energy-storage elements can be divided into the battery and supercapacitor types. One of the most important tasks in the development of energy-storage elements with considerable specific characteristics is the combination of the maximum stored energy and its power. In the current work we present the results of the elaboration and characterization of a nanostructured carbon material with excellent energy-storage properties.

In order to achieve a high specific capacity, carbon materials with a high specific surface and electron conductivity, such as absorbent carbons, graphite tissue, nanotubes, nanoporous carbon, etc. [1] are currently used as electrodes. The key factors in the choice of such materials are the specific surface area, the geometry of the pores and their size distribution, the average pore size, and the wettability and electrolyte conductivity in the pores, as well as the presence of electroactive particles at the surface.

Recent investigations have shown that increasing the specific surface allows one to reach specific-capacity values for carbon-based supercapacitors up to 50 F/g. A further increase in capacity has not been observed even in the most porous samples [2]. This is due to the fact that a decrease in the pore size favors an increase in the diffusion resistance of a material.

In connection with this, researchers have a large interest in carbon nanostructures, in particular, quasi-one-dimensional nanotubes. On the one hand, they possess a high specific surface at a very high level of conductivity; on the other hand, they have low ion diffusion coefficients through the nanotube wall, which impedes the penetration of electrolyte ions into the material during charging.

One review [3] referenced the works with an original explanation of the high electrochemical activity of nanostructured carbon, which is caused by the low work functions of linear and quasi-linear fragments of structures. Our research group found an anomalously high intensity of the cold emission of electrons from the surface of amorphous linear chain carbon [4], which indicates the low effective work function of this material and, consequently, the prospects of its application in electrochemical energy-storage elements.

Nanostructured materials on the basis of low-dimensional carbon forms can thus be considered as the most promising systems for electrodes of energy-storage elements with excellent specific characteristics.

This work is aimed at studying the effect of the structural characteristics of nanocarbon material on the specific supercapacity of a supercapacitor that is constructed on its basis.

THE SYNTHESIS AND ACTIVATION OF THE STUDIED NANOCARBON MATERIAL

The carbon material that was used in this work was obtained in the form of cotton via chemical dehydrohalogenation of polyvinylchloride (PVC) and polyvinilidenchloride (PVDC) copolymer fibers [5]. It was activated via the thermal and chemical methods. To carry out electrochemical studies, the samples were ground in a ball mill under an argon atmosphere to a micron size in order to obtain fine powders; they were then were applied to metallic electrodes.

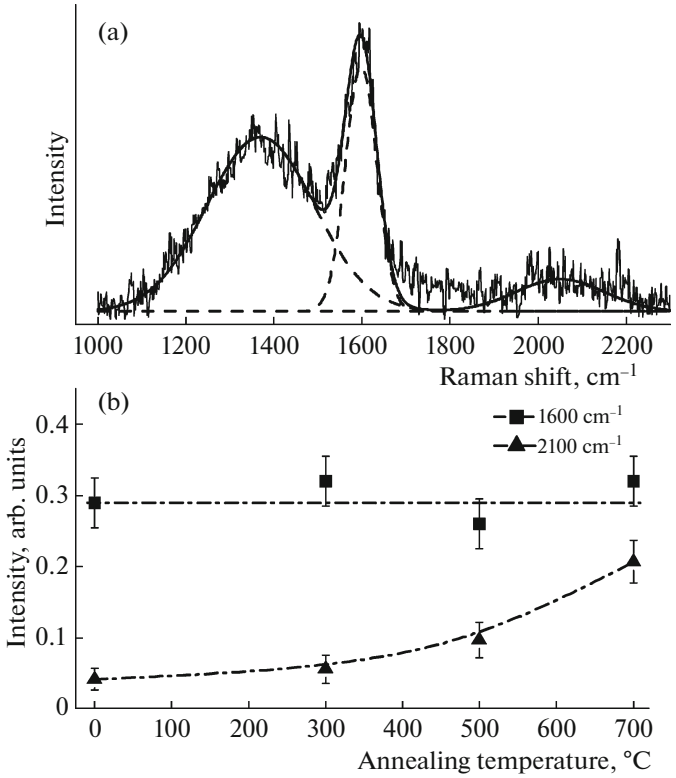

Fig. 1. (a) The typical Raman spectrum of a nanocarbon material; (b) the dependence of the relative contribution of graphite-like and chain components in the material structure on the temperature of annealing.

Annealing was performed in two stages. In the first one, the samples were annealed in air at a temperature of up to 300°C, which resulted in desorption of the residual products of a chemical reaction without structural changes in the material. In the second one, the same samples were annealed in an argon atmosphere at various temperatures with a step of 100°C up to 700°C, which led to structural modification with the formation of linear chain carbon fragments.

The chemical activation of the nanocarbon material was achieved in two ways: i) via treatment in nitric acid at a temperature of 50°C and ii) exposure in a concentrated sodium hydroxide solution for 1 day with subsequent stage annealing (first at 500°C for half an hour and then at 700°C for half an hour). The samples were thoroughly washed in order to remove the residual reagents of the chemical activity. The best results on the specific capacity were obtained after activation in sodium hydroxide.

PROBING OF NANOCARBON MATERIALS

The structure of the studied nanocarbon material was identified via electron microscopy, X-ray microanalysis, Raman spectroscopy, Auger electron spectroscopy, electron spectroscopy for chemical analysis (ESCA), and electron energy–loss spectroscopy.

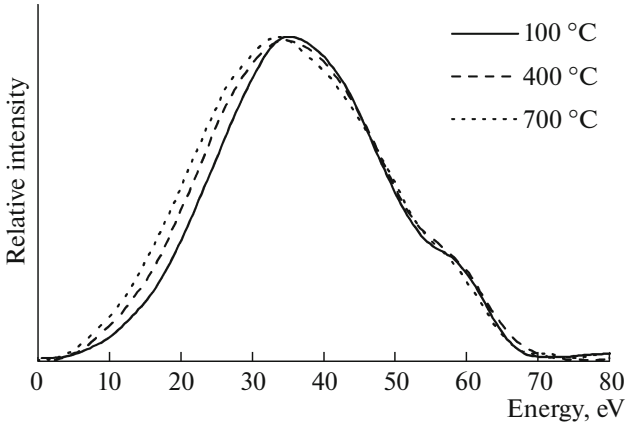

Fig. 2. The integral Auger spectra of the studied samples after annealing at various temperatures.

EXPERIMENTAL RESULTS AND DISCUSSION

Studies of the chemical compositions of the samples via X-ray microanalysis and ESCA revealed that dehydrohalogenation and annealing make the material almost carbonaceous (the carbon atomic fraction exceeds 95%). The electron microscopy results for this nanocarbon material after thermal annealing at 400°C revealed a decrease in the average fiber diameter by approximately 2 times. The specific surface of this material as measured by the Brunauer–Emmett–Teller method is 550 m^2/g. The conductivity of the carbon fiber grows with increasing annealing temperature from 0.13×10^{-6} S/cm at 300°C to 0.59 S/cm at 700°C.

Figure 1a displays the typical Raman spectrum of the studied nanocarbon material. Three characteristic lines are observed: a peak near 1600 cm^{-1} that corresponds to the graphite-like structure; a wide peak at 1300–1400 cm^{-1}, which is usually attributed to nanostructured graphite [6], and a line at 2000–2200 cm^{-1} from cumulene and polyyne chain structures [7]. To determine the contribution of any structural component, the Raman spectra were decomposed into Gaussian curves. The fraction of various components was calculated from the Gaussian area. Figure 1b shows the dependence of the relative contribution of the graphite-like and chain components on the temperature of annealing. As is obvious from the plot, the graphite-like component fraction is almost unchanged and the half-width of this peak is also constant. The contribution of the chain component increased by 5 times with increasing annealing temperature. The major growth of this peak begins at temperatures above 300°C. Here, conductivity increases by 2 orders of magnitude after annealing over the temperature

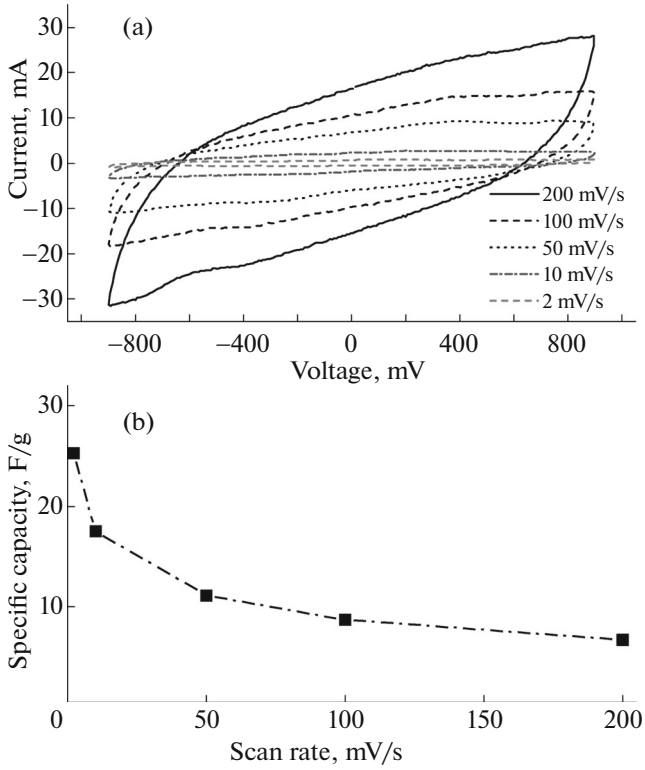

Fig. 3. (a) Cyclic voltammograms of the sample after annealing at 700°C in an argon atmosphere at various scan rates; (b) the dependence of the specific capacity on the scan rate.

range of 500–700 °C, which is probably due to the increasing contribution of chain structures and the ordering of the graphite-like component. It is worth mentioning that the contribution of nanostructured graphite decreases with increasing annealing temperature, which can be explained by an increase in the crystallite size [6].

Figure 2 depicts the integral Auger spectra of the samples after annealing at various temperatures (the energy is calculated from the Fermi level). As is seen, at increasing temperatures of annealing the low-energy edge of the spectrum is shifted toward the Fermi level. This indicates the increased density of electron states near the Fermi level, which explains the growth of conductivity during annealing.

The electrochemical characteristics of the studied carbon material were measured in accordance with a two-electrode scheme via cyclic voltammetry on an Elins P-150 potentiostate. A sodium hydroxide water solution (6 M KOH) was used as the electrolyte. The typical voltammograms of the samples after annealing are shown in Fig. 3a. Figure 3b displays the specific capacity as a function of the scan rate calculated from the relevant voltammograms. As is seen from the plot, the specific capacity is increased by 3.5 times with decreasing scan rate, which is due to the high content

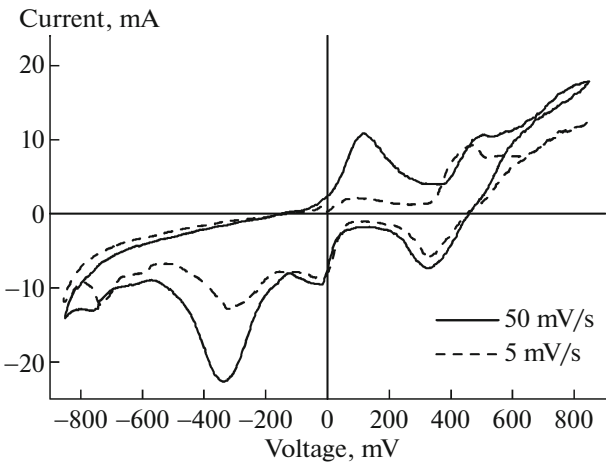

Fig. 4. Cyclic voltammograms of the material that was activated in KOH at scan rates of 5 and 50 mV/s.

of nanopores in the material, whose small diameters limit the ion diffusion of the electrolyte. It follows that the specific capacity value of our material is determined by its ionic conductivity with an intercalation (diffusive) mechanism rather than by conductivity. The slope of cyclic voltammograms, which also decreased with decreasing scan rate, confirms the determining contribution of ionic conductivity.

The measurement of the specific capacity of the material after annealing at different temperatures revealed a pronounced increase in capacity after annealing at 700°C (6 F/g after 400°C and 25 F/g after 700°C). This result can be explained by the growing conductivity of the material after annealing. These specific capacity values are typical of activated carbon, whose chemical activation leads to an additional increase in capacity; it was shown in [8] that activation in sodium hydroxide leads to an increase in specific capacity from 30 to 47 F/g.

In connection with this, we carried out experiments on the effects of chemical activation on the capacity characteristics of the studied material. Figure 4 displays the cyclic voltammograms of the material that was activated in KOH. The specific capacities that were calculated from the appropriate voltammograms were 9.7 F/g and 100.7 F/g at a scan rate of 50 mV/s and 5 mV/s, respectively. It is worth mentioning that at a high scan rate the specific capacities of the chemically activated and inactivated materials are almost the same, while at a low scan rate the activated material possesses a capacity that is 4 times higher. This may be explained if the chemical treatment of the nanopores did not occur earlier.

The table shows the summarized results of the electrochemical experiments. It follows from these that attaining a high power capacity of the material requires its annealing at a high temperature, viz., 700°C. As a result, the specific capacity increased by 5 times.

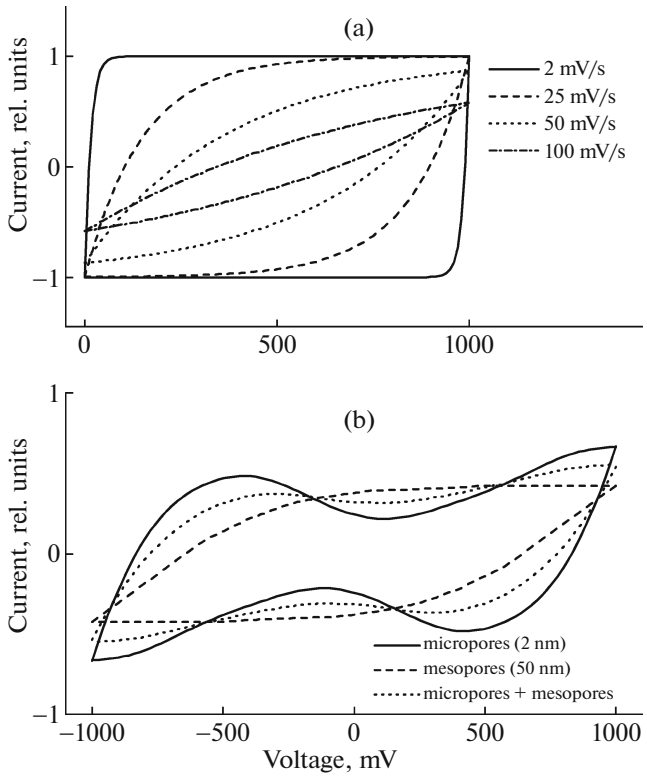

Fig. 5. (a) Calculated voltammergoramms of an electrochemical cell at various scan rates; (b) calculated voltammograms of an electrochemical cell with microporous, mesoporous and mixed electrodes.

Chemical activation led to an additional fourfold increase in the specific capacity.

THEORETICAL ANALYSIS AND MODEL CALCULATIONS

To explain the experimental results, we simulated the voltamerogramms while considering two parameters: the conductivity of the material and its pore sizes. The simulation was conducted in accordance with the technique that was proposed in [9]. For an ideal voltammogram the applied voltage V_t (without polarization) at the time t is written as

$$V_t = V_1 \pm v \cdot t,$$

where V_1 is the initial voltage and v is the scan rate.

With a significant internal resistance, R, that is related to the limited diffusion of ions in pores and between crystallites, a voltage drop, IR, occurs. Then

$$V_t = V_1 + vt - IR, \quad \text{at} \quad 0 < t < V_2 / v,$$
$$V_t = V_1 - vt - IR, \quad \text{at} \quad V_2 / v < t < 2V_2 / v,$$

where V_2 is the maximum voltage range.

Differentiating these equations with respect to time and resolving them according to the conditions

$$I_+(0) = I_-\left(\frac{2V_2}{v}\right) \quad \text{and} \quad I_+\left(\frac{V_2}{v}\right) = I_-\left(\frac{V_2}{v}\right),$$

we obtain the following equations for the positive, I_+, and negative, I_-, currents:

$$I_+(V) = Cv - \left(\frac{2vC}{1+\exp\left(\frac{V_2}{vRC}\right)}\right)\cdot\exp\left(-\frac{t}{RC}\right),$$
$$\text{at} \quad 0 < t < V_2 / v,$$
$$I_-(V) = -Cv$$
$$+\left(\frac{2vC}{\exp\left(-\frac{V_2}{vRC}\right)\left(1+\exp\left(-\frac{V_2}{vRC}\right)\right)}\right)\cdot\exp\left(-\frac{t}{RC}\right),$$
$$\text{at} \quad V_2 / v < t < 2V_2 / v.$$

Figure 5 displays the calculated charge and discharge currents ($I(V)/vC$) for various scan rates, v, depending on the external measured voltage ($V_m = V_t + IR$) on a cell with the parameters $R = 75\ \Omega$, $C = 0.1$ F, and $V_2 = 1$ V. As follows from the figure, at a low scan rate the current is small enough so that the IR losses are insufficient and the voltammogram is substantially in agreement with that of an ideal capacitor. When the scan rate is increased, the current increases, and IR losses become significant. This results in a decrease in the current; the voltammogram, which exhibits a "capacitative" form at low v, becomes more resistive with an increase in v. At very high scan rates the voltammogram tends to the purely resistive form, which has a linear dependence.

A capacitor of a material that has varying pore sizes can be presented as the parallel connection of mesoporous and microporous capacitors with the C_a and C_b capacities, respectively. The diameter of the micropores is assumed to be less than 2 nm, while the mesopore size is between 2 and 50 nm.

With a linear potential sweep the dependence of the current through each capacitor on the time t is expressed as follows:

$$I_a(V) = C_a v + \left(\frac{V_1}{R_a} - vC_a\right)\exp\left(\frac{-t}{R_aC_a}\right), \qquad (1)$$

$$I_b(V) = C_b v + \left(\frac{V_1}{R_a + R_b} - vC_b\right)\exp\left(\frac{-t}{(R_a + R_b)C_b}\right). \qquad (2)$$

If the scan time t is greater than R_aC_a, the exponential side of Eq. (1) tends to zero and Eq. (1) thus has the form $I_a = vC_a$.

Since the diffusion of ions in micropores occurs much more slowly than in the mesopores, the resis-

tance of micropores will be much greater, compared to that in mesopores ($R_0 \gg R_a$). As well, the micropore surface area is typically higher than for mesopores, which results in the total capacities $C_b \gg C_a$.

If the time t is small (at a high scan rate) in comparison with R_bC_b, the exponential part of Eq. (2) can be assumed to be 1. Then I_b tends to zero and the total measured current is simply I_a. The direct current can be used at this stage for the measurements of mesoporous capacity without considering the microporous capacity.

In another extreme case, where t is high (slow scan rate) in comparison with R_bC_b, both exponential terms in Eqs. (1) and (2) equal zero and Eq. (2) is expressed as $I_b = vC_b$, while the total measured current is $I_a + I_b = v(C_a + C_b)$.

The C_a and C_b capacities can be obtained separately by measuring the total current at high and low scan rates. As is obtained by theoretical analysis and modeling (Fig. 5*b*), the cyclic voltammerometry allows one to calculate various characteristics and parameters of supercapacitors.

It can be concluded from the modeling results that reducing the conductivity of the electrode material leads to the distortion of the voltammogram, which is ideal for a capacitor (the rectangular type). It manifests itself in the emergence of the characteristic slope, which grows with increasing resistance. The opening of nanopores that is caused by chemical activation leads to the appearance of symmetrical maxima in the voltammogram.

CONCLUSIONS

A nanostructured carbon material with excellent energy-storage properties was obtained and characterized in this work. The results of the studies revealed that the energy capacity of this material was defined by not only its specific surface, but also by its structural features. In order to increase the specific capacity, various thermal and chemical activation methods were applied to the studied nanocarbon material. It was shown that with thermal activation the quasi-one-dimensional carbon fraction increased with an increase in the temperature of annealing. In addition to the charge accumulation due to the formation of an electric double layer at the surface, obtaining the maximum power capacity of the material required the activation of intercalation processes in the pores.

REFERENCES

1. P. Simon and Y. Gogotsi, Nat. Mater. **40** (7), 2596 (2008).
2. V. V. N. Obreja, Phys. E **40** (7), 2596 (2008).
3. A. G. Krivenko and N. S. Komarova, Russ. Chem. Rev. **77**, 927 (2008).
4. V. G. Babaev, V. V. Khvostov, M. B. Guseva, N. F. Savchenko, and Yu. Belokoneva, Poverkhnost, No. 5, 89 (2007).
5. A. F. Aleksandrov, V. G. Babaev, M. B. Guseva, et al., RF Patent No. 2261944 (2005).
6. P. Mallet-Ladeira, P. Puech, et al., Carbon **80**, 629 (2014).
7. L. Ravagnan, F. Siviero, C. Lenardi, et al., Phys. Rev. Lett. **89**, 285506 (2002).
8. M. Natalia, Y. N. Sudhakar, and M. Selvakumar, Indian J. Chem. Technol. **20**, 392 (2013).
9. W. G. Pell and B. E. Conway, J. Electroanal. Chem. **500**, 121 (2001).
10. A. J. Bard and L. R. Faulkner, *Electrochemical Methods: Fundamentals and Applications* (Wiley, New York, 1980).

Translated by O. Maslova